

The effect of the particle concentration in biocompatible magnetic fluids: A dynamical susceptibility investigation

P.C. Morais*, J.G. Santos, L.B. Silveira, A.C. Oliveira

Universidade de Brasília, Instituto de Física, Núcleo de Física Aplicada, 70919-970 Brasília, DF, Brazil

Available online 12 October 2006

Abstract

Room-temperature measurements of the imaginary component of the susceptibility of magnetic nanoparticles in biocompatible magnetic fluids have been carried out in this study. We investigated the susceptibility peak position of surface-coated magnetic nanoparticles as a function of the particle concentration in the range of 10^{14} to 10^{16} particle/cm³. Magnetite nanoparticles were surface-coated with dextran and dimercaptosuccinic acid before peptization as biocompatible magnetic fluids. Analyses of the imaginary susceptibility curves, in the limit of zero external fields, include both the particle size polydispersity profile and particle–particle interaction.

© 2006 Elsevier B.V. All rights reserved.

Keywords: Biocompatible magnetic fluid; Precipitation; Dynamical susceptibility; Magnetic measurements

1. Introduction

In recent years the design and synthesis of biocompatible magnetic fluids has attracted intense interest, with special emphasis on their applications in biomedicine [1,2]. This study reports on magnetic investigation of dextran and dimercaptosuccinic acid (DMSA)-coated magnetite-based biocompatible magnetic fluids using initial dynamical susceptibility (DS) measurements. Here, special emphasis is devoted to the concentration dependence of the susceptibility peak frequency (imaginary component), in the limit of zero external fields. The susceptibility peak frequency behaviour is a key aspect for magnetohyperthermia with application in cancer therapy [3].

2. Experimental results and discussion

The biocompatible magnetic fluid (BMF) samples were prepared according to the standard procedure described in Ref. [4]. The samples were diluted to produce five particle concentrations in the range of 10^{14} to 10^{16} particle/cm³. The transmission electron (TEM) micrographs of the surface-coated magnetite nanoparticles samples were recorded using a JEOL-1010 system. The particle size histograms obtained from the TEM data were curve-fitted using the lognormal distribution function. The average particle diameter (diameter dispersion) obtained from the TEM data were 3.1 nm (0.26) and 5.6 nm (0.22) for the dextran-coated and DMSA-coated magnetite nanoparticles, respectively.

The room-temperature DS measurements (real and imaginary components), in the limit of zero external fields (initial susceptibility), were carried out using a home-made Robinson oscillator operating in the MHz region (14–38 MHz). Such experimental setup has been successfully used to investigate magnetic nanoparticles dispersed in polymeric-based composites [5,6]. The description of the imaginary component (χ'') of the zero-field DS curve is based on the model discussed by El-Hilo et al. [7]. The model allows one to include the particle–particle interaction via the effect of the particle concentration upon the imaginary susceptibility component. Shortly, the initial susceptibility curve description is provided by

$$\chi'' = A \int_0^{V_b} g(\omega, T) V f(V) dV + B \int_{V_b}^{\infty} g(\omega, T) f(V) dV + C \int_0^{\infty} g(\omega, T) V^3 f(V) dV, \quad (1)$$

with $g(\omega, T) = \omega \tau_0 \exp(\beta KV) / [1 + \omega \tau_0 \exp(\beta KV)]$. A , B and C are parameters obtained from the fitting of the frequency-dependence of the zero-field DS curves. The first two integral in Eq. (1) account for non-interacting nanoparticles as follows. The first integral describes the contribution due to the superparamagnetic particles whereas the second integral accounts for the blocked nanoparticles. The third integral on the right-hand side of Eq. (1) represents the contribution to the initial susceptibility due to the dipolar interactions. The particle volume polydispersity profile of the samples is accounted for by the lognormal distribution function $f(V)$, whereas $g(\omega, T)$ describes the Debye approximation with $\beta = 1/kT$.

The relaxation of the nanoparticle magnetic moment for uniaxial anisotropy is given by [5,8]:

$$f = f_0 \exp\left(\frac{-\Delta E}{kT}\right), \quad (2)$$

* Corresponding author. Tel.: +55 61 32736655; fax: +55 61 32723151.
E-mail address: pcmor@unb.br (P.C. Morais).

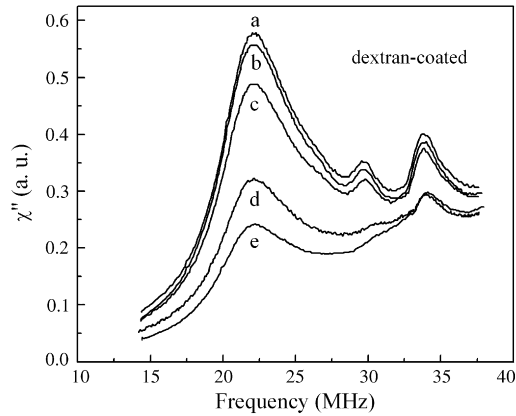


Fig. 1. Zero-field imaginary components of the dynamical susceptibility. Curves labelled (a), (b), (c), (d), and (e) correspond to the dextran-coated MF samples containing 4.8×10^{16} , 2.4×10^{16} , 9.6×10^{15} , 4.8×10^{15} , and 4.8×10^{14} particle/cm³, respectively.

where $\Delta E = KV + \alpha\mu^2c$ is the height of the energy barrier. The first term in ΔE describes the effective anisotropy energy, whereas the second term in ΔE describes the dipolar interaction energy. The dipolar coupling constant, particle magnetic moment, and particle concentration are described by α , $\mu = M_S V$, and c , respectively.

Figs. 1 and 2 show the imaginary components (zero-field data) of the susceptibility (DS) of dextran- and DMSA-coated magnetite nanoparticles dispersed as MF samples, respectively. The nanoparticle concentration for both samples was varied in the range of 10^{14} to 10^{16} particle/cm³. Note from Figs. 1 and 2 the presence of three well-defined DS peaks around 22, 31, and 35 MHz named P1, P2, and P3, respectively. In addition, note that all the DS peaks show a tendency to shift to higher frequencies upon dilution (top to bottom) of the MF sample.

Symbols in Fig. 3 represent the DS peak positions P1–P3 as a function of the nanoparticle concentration, respectively. Using Eq. (1) the peak positions were obtained by fitting the three structures observed in the imaginary components of the DS susceptibility curves shown in Figs. 1 and 2.

Solid lines in Fig. 3 represent the best fit of the data according to Eq. (2). Note from Fig. 3 that the data related to the dextran-coated (\blacktriangle) nanoparticles are always running below the data related to the DMSA-coated (\bullet) nanoparticles. According to Eq. (2) this finding indicates a difference in the effective anisotropy energy (KV) between the two samples. As the average particle diameter of magnetite surface-coated with dextran (3.1 nm) is smaller than the average particle diameter of the DMSA-coated magnetite (5.6 nm) the effective anisotropy constants of the two samples are quite different. From the fitting of our data we found

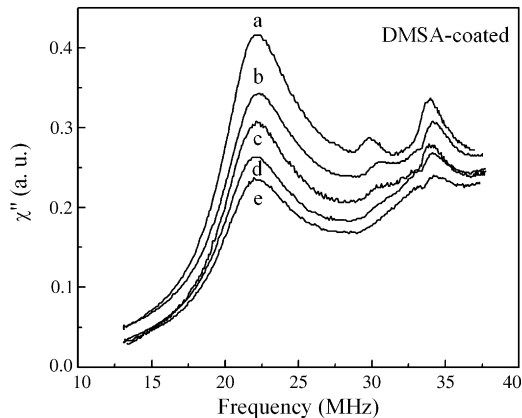


Fig. 2. Zero-field imaginary components of the dynamical susceptibility. Curves labelled (a), (b), (c), (d), and (e) correspond to the DMSA-coated MF samples containing 4.9×10^{16} , 2.4×10^{16} , 9.6×10^{15} , 4.9×10^{15} , and 4.9×10^{14} particle/cm³, respectively.

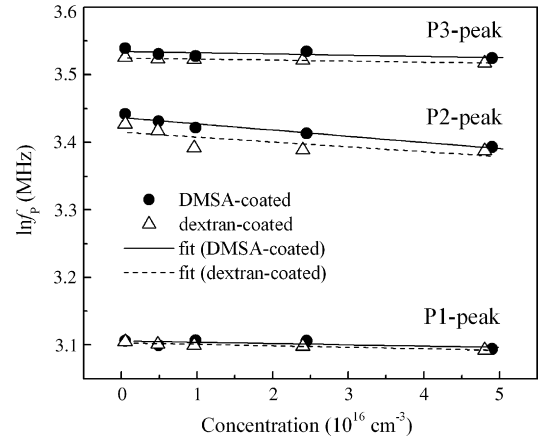


Fig. 3. Peak frequency vs. nanoparticle concentration. Symbols represent the best fitted values of the peak positions (P1–P3) for the DMSA-coated (\bullet) and dextran-coated (Δ) samples. Solid (DMSA-coated) and dashed (dextran-coated) lines represent the best fitting of the data using Eq. (2). Note the vertical logarithmic scale.

the values of 4.6×10^5 and 7.8×10^4 J/m³ for the effective anisotropy constant of the dextran-coated and DMSA-coated magnetite nanoparticles. Such difference in the effective anisotropy values could be due to both the difference in the surface-coating species and different contributions due to surface anisotropy. The anisotropy constant of bulk magnetite is about 1.9×10^4 J/m³ [9].

Besides dynamic susceptibility, magnetic resonance has been extensively used as an important tool in the investigation of different aspects related to magnetic fluids [10]. Magnetic resonance allows investigation of the effective anisotropy (K) of magnetic nanosized particles in terms of bulk (K_b) and surface (K_s) components, i.e. $K = K_b + K_s$ [11]. The anisotropy surface component scales with the nanoparticle diameter (D) according to $K_s = (6/D)k_s$, where k_s is an anisotropy surface coefficient [12] which is not only temperature dependent, but also dependent upon the particle structure and surface-coating. The ratio of the values we found for the surface anisotropy component ($K_s = K - K_b$) scales with the particle size as $(K_s^{\text{dextran}}/K_s^{\text{DMSA}}) = (D^{\text{DMSA}}/D^{\text{dextran}})^\alpha$, with $\alpha \approx 3.3$. Superlinear values of α ($\alpha > 1$) indicate the influence of the nanoparticle surface coating upon the surface anisotropy.

3. Conclusion

In summary, dynamic susceptibility measurements were used to investigate magnetite-based biocompatible magnetic fluid samples. Two distinct surface-coating molecular species were used to produce the magnetic fluid samples, namely dextran and dimercaptosuccinic acid. Three well-resolved peaks were identified in the imaginary susceptibility curves. The peak positions were investigated as a function of the particle concentration in the range of 10^{14} to 10^{16} particle/cm³. The susceptibility imaginary component analyses took into account the superparamagnetic particles, the blocked particles, particle–particle interactions, and the particle size polydispersity profile. Our investigation shows a huge difference between the effective anisotropy constants of the two samples. We found values of 4.6×10^5 and 7.8×10^4 J/m³ for the effective anisotropy constant of the dextran-coated and DMSA-coated magnetite nanoparticles, respectively. These values are different from one another and from the bulk value (1.9×10^4 J/m³). Such difference in the effective anisotropy values could be due to both the difference in the surface-coating species and different contributions due to surface anisotropy.

Acknowledgements

This work was partially supported by the Brazilian agencies FINATEC and CNPq.

References

- [1] C.C. Berry, A.S.G. Curtis, *J. Phys. D: Appl. Phys.* 36 (2003) R198–R206.
- [2] M.H.A. Guedes, M.E.A. Guedes, P.C. Morais, M.F. da Silva, T.S. Santos, J.P. Alves Jr., C.E. Bertelli, R.B. Azevedo, Z.G.M. Lacava, *J. Magn. Magn. Mater.* 272–276 (2004) 2406–2407.
- [3] M.H.A. Guedes, N. Sadeghiani, D.L.G. Peixoto, J.P. Coelho, L.S. Barbosa, R.B. Azevedo, S. Kückelhaus, M.F. Da Silva, P.C. Morais, Z.G.M. Lacava, *J. Magn. Magn. Mater.* 293 (2005) 283–286.
- [4] T. Goetze, C. Gansau, N. Buske, M. Roeder, P. Gornert, M. Bahr, *J. Magn. Magn. Mater.* 152 (2002) 399–402.
- [5] A.F.R. Rodriguez, A.C. Oliveira, P.C. Morais, D. Rabelo, E.C.D. Lima, *J. Appl. Phys.* 93 (2003) 6963–6965.
- [6] L.B. Silveira, J.G. Santos, A.C. Oliveira, A.C. Tedesco, J.M. Marchetti, E.C.D. Lima, P.C. Morais, *J. Magn. Magn. Mater.* 272–276 (2004) 1195–1196.
- [7] M. El-Hilo, K. O'Grady, R.W. Chantrell, *J. Magn. Magn. Mater.* 114 (1992) 295–306.
- [8] L. Néel, *C.R. Acad. Sci.* 228 (1949) 664–666.
- [9] B. Payet, D. Vincent, L. Delaunay, G. Noyel, *J. Magn. Magn. Mater.* 186 (1998) 168–174.
- [10] P.C. Morais, F.A. Tourinho, G.R.R. Gonçalves, A.L. Tronconi, *J. Magn. Magn. Mater.* 149 (1995) 19.
- [11] G.R.R. Gonçalves, A.R. Pereira, A.F. Bakuzis, P.C. Morais, F. Pelegrini, K. Skeff Neto, *J. Magn. Magn. Mater.* 226 (2001) 1896.
- [12] O. Silva, E.C.D. Lima, P.C. Morais, *J. Appl. Phys.* 93 (2003) 8456.